Powder Metallurgy and Metal Ceramics, Vol. 50, Nos. 5-6, September, 2011 (Russian Original Vol. 50, Nos. 5-6, May-June, 2011)

THEORY AND TECHNOLOGY OF SINTERING, THERMAL AND CHEMICOTHERMAL TREATMENT

SELECTIVE LASER SINTERING/MELTING OF NITINOL–HYDROXYAPATITE COMPOSITE FOR MEDICAL APPLICATIONS

I. V. Shishkovskii,[1,2] I. A. Yadroitsev,[1] and I. Yu. Smurov[1]

UDC 621.373.826:621.762.53

The layer-by-layer synthesis of 3D parts from nitinol (NiTi intermetallide) and hydroxyapatite additions using selective laser sintering/melting (SLS/SLM) is studied. The effect of different laser parameters on the structure and phase composition of sintered/melted samples is analyzed with optical and scanning electron microscopy, x-ray diffraction, and energy-dispersive x-ray analysis. Optimum SLS/SLM parameters are determined for the synthesis of NiTi + HA to be used in tissue engineering and manufacture of medical devices (pins, nails, porous implants, drug delivery systems). No significant destruction of HA ceramics under laser treatment is observed. The amount of nickel released to the surface of 3D parts decreases owing to the additional oxidation of free titanium during SLS/SLM and the formation of a protective HA layer. Full-density 3D parts are produced from nitinol by SLM including preheating to 300°C.

Keywords*: selective laser sintering/melting (SLS/SLM), porous tissue engineering, nitinol, hydroxyapatite (HA).*

INTRODUCTION

Nitinol (NiTi intermetallic phase) is a promising implant material due to its unique combination of properties: high strength and corrosion resistance, shape memory effect and biocompatibility [1–3]. Moreover, NiTi possesses these properties when in the porous state. Open porosity is extremely useful for connective tissue–implant bonding to ensure, along with mechanical fixation, additional biological fixation of the implant to the bone.

Selective laser sintering/melting (SLS/SLM) in combination with computer 3D x-ray tomography and/or magnetic resonance spectroscopy allows porous cell tissue (engineering tissue) scaffolds to be produced from nitinol to closely conform to the identify of the patient's organs (bones) being reconstructed, which is a huge advantage of this technique. However, the use of such implants in the long term requires further research [4–6]. Physicians are especially concerned about the potential release of nickel from the intermetallic NiTi phase, which causes severe toxicity in humans. This may occur under a thermal effect on nitinol or because of its corrosion in the

[1]Lebedev Physical Institute, Russian Academy of Sciences, Samara Branch, Samara, Russia.

[2]To whom correspondence should be addressed; e-mail: shiv@fian.smr.ru.

Translated from Poroshkovaya Metallurgiya, Vol. 50, No. 5–6 (479), pp. 35–46, 2011. Original article submitted November 11, 2009.

implantation area. A solution to this problem may be to deposit an additional biocompatible coating over the nitinol surface.

Ceramics based on hydroxyapatite (HA), $Ca_{10}(PO_4)_6(OH)_2$, are a well-known biocompatible material used for coating of metal prosthetic components and as an actual implant material [7–11]. The chemical structure of HA is close to the mineral phase of bone tissues. There are studies on the use of SLS to produce bioresorptive implants (i.e., those that are resorbed or replaced with bone during some time) from ceramic polymers (ε-polycaprolactam + HA, polyvinyl + HA, polyethylketone + HA, HA derivative—tricalcium phosphate nanoparticles filled with poly-(hydroxybutyrate/hydroxyvalerate). The structures (scaffolds) of these ceramic polymers with premodeled architecture of internal and external surfaces are also attractive for tissue engineering. Moreover, no significant effect of the HA amount in an implant on the surface shape and roughness has been revealed. However, additions of HA ceramics decrease the strength of parts. On the other hand, the presence of HA on the surface influences the hydrophobic behavior and improves wettability. It is important to note that HA coatings block the pores and smooth out the effect of nickel present in NiTi parts [5].

Plasma deposition and pulsed laser deposition [12, 13] are most popular methods for HA application to nitinol surface. However, with these methods, HA powder is heated actually to the evaporation temperature to settle on a nitinol substrate. These HA deposition methods are disadvantageous mainly because they involve poor reproducibility and poor control of the phase composition of a material deposited in experiments *in vitro* and *in vivo*. The variation in the morphology and phase composition of HA deteriorates the mechanical and biological stability of the ceramics. With high-temperature HA deposition, the coating contains metastable (prone to decomposition) phases that reduce the biocompatibility and adhesion between the coating and surrounding bone tissues. It is reported in [2, 14] that high-temperature sintering decreases the Ca/P ratio in HA, actually characterizing biocompatibility, and oxide phases precipitate from the ceramics.

The paper [2] shows the possibility of forming a hydroxyapatite layer over nitinol using SLS of a HA + NiTi powder mixture. The bioactivity and biocompatibility of implants produced with this technique are high [3]. Moreover, in accordance with the concept of functionally gradient materials developed in [15], additive laser sintering allows the amount of HA and the future porosity and permeability of a part to be controlled, thus, improving its osteoconductivity.

This study is intended to conduct SLS/SLM of both pure nitinol (NiTi) and a HA + NiTi mixture and to examine the effect of laser parameters on the microstructure and phase composition of the material using optical and scanning electron microscopy (SEM), x-ray diffraction, and energy-dispersive x-ray analysis. Another objective is to ascertain the contribution of hydroxyapatite to the potential decomposition of the NiTi phase during SLS/SLM and to smoothing the effect of nickel released during high-temperature laser treatment.

MATERIALS AND EQUIPMENT

For the experiments conducted at the National School of Engineering (Saint-Étienne, France), nitinol powder containing 99.76 wt.% intermetallic NiTi phase and hydroxyapatite (HA) powder containing 99.5 wt.% $Ca_{10}(PO_4)_6(OH)_2$ were used, both powders being produced by the TLS Technik GmbH&Co. The NiTi powder was represented by a 45 μm fraction and the HA powder by a 2 to 10 μm fraction. The NiTi phase was obtained by gas-phase atomization. The stoichiometry of NiTi was complied with: Ni balance and 45 wt.% Ti. The particle size distribution was determined with an ALPAGA 500NANO (OCCHIO s.a.) granulometer: $d_{10} = 11.4$ μm, $d_{50} =$ $= 25.5$ μm, and $d_{90} = 37.5$ μm.

For the sintering experiments at the Samara Branch of the Physical Institute (Russian Academy of Sciences), nitinol powder of PN55T45 grade (produced by the Polema Company, Tula, Russian Federation) and hydroxyapatite powder of GAP85d grade (as per medical standard VFS 42-2378–94) were used. The powders had the following composition: PN55T45 nitinol powder contained 55% nickel and 45% titanium and the HA powder contained 99.6 wt.% $Ca_{10}(PO_4)_6(OH)_2$. The particle size (~100 μm) of the two powders was selected with a sieve analysis to match the diameter of the laser spot.

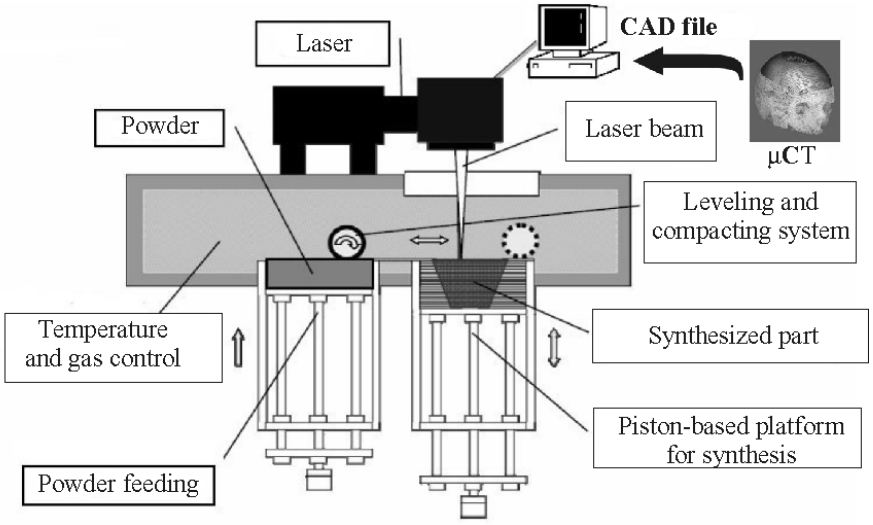

Fig. 1. Schematic of the SLM process using a Phenix Systems PM-100 Setup

Note that the ratio of components in the Ni–Ti system is strictly determined by the stoichiometry of the synthesized compound, NiTi intermetallic phase, while the amount of HA sufficient for its pharmacological properties to show up is not found in the literature [2, 10]. To compare the results of NiTi layer-by-layer synthesis and data on the effect of HA additions, a mixture of NiTi and HA in the ratio 4 : 1 and the above powders without HA were subjected to laser treatment.

A Phenix Systems PM-100 setup for SLS/SLM (Fig. 1) used at the National School of Engineering (Saint-Étienne, France) includes: a continuous-operation laser; deflectors for scanning laser radiation in the *X*–*Y* plane; a personal computer to control the process, where relevant software is used to cut models of the automatic design system into layers; a roller mechanism for applying and leveling a powder mixture; two cylindrical platforms (pistons) with adjustable (up to several micrometers) movement in the vertical direction. The left piston (Fig. 1) contains the starting powder mixture and the right piston is designed for layer-by-layer synthesis of a 3D part. Sintering can proceed in air or nitrogen or argon at high or low ambient temperatures. The PM-100 setup is advantageous in that the powder can be heated to 900°C during layer-by-layer synthesis, which is important in dealing with high-temperature ceramics. We used this advantage in our study. After a single layer is sintered, the platforms synchronously move (the left platform goes up and the right one down) by the thickness of the layer sintered and the roller evenly distributes the starting powder from the left piston over the right platform and the process is repeated until a 3D part is finished. The unused powder 'supports' the part during its production, on the one hand, and can be used once again (i.e., this is a wasteless technology), on the other. If laser power is high, sintering transforms into melting. When powders with different melting points are sintered, liquid-phase sintering proceeds, in which the fusible phase fills the pores of the refractory phase [16, 17].

The PM-100 setup is equipped with an IPG Photonics YLR-50 fiber laser with the maximum power P = = 50 W, laser wavelength 1075 nm, and spot diameter $d \sim 70$ μm. The powder is distributed with the roller on the platform 100 mm in diameter. The laser power and scanning rate, the spacing between passes of the laser beam, temperature, and the composition of the powder mixture and gas environment in the layer-by-layer chamber are variable parameters.

The experimental setup for SLS of powder compositions used at the Samara Branch of the Physical Institute (Russian Academy of Sciences) includes: a continuous-operation YAG : Nd^{+3} laser (Kvant-60); a deflector for scanning laser radiation in the *X*–*Y* plane; a personal computer to control the process; replaceable focusing lenses to ensure the focal spot 50 and 100 μm in diameter; a mechanism for applying and leveling the powder mixture; and a cylindrical platform moving in the vertical direction. In the experiment, the laser power was varied from 2 to 30 W, the beam scanning rate V changed over a wide range, and the diameter of the focal spot was about

100 μm. The samples of single layers and 3D parts were sintered in a specially designed chamber in argon atmosphere. The experimental setup, SLS technique, and optimal conditions for sintering of NiTi were described previously in [1].

The main feature of the SLS technique implemented at the Samara Branch of the Physical Institute, distinguishing it from proprietary processing units (3D Systems Co., EOS GmbH, Phenix, etc.), is that no force is induced to level the powder mixture over the surface to be sintered and laser wavelength $\lambda = 1.06$ μm is used. The process if semiautomatic, so another important advantage is that synthesis may be interrupted at any time, which is beneficial in a search for optimal conditions.

The sintering resulted in porous and full-density flat single-layer samples approximately $10 \times 10 \times d$ (mm) in size, where d is the thickness of a single layer.

The macrostructure was examined with an Olympus BX60M optical microscope with a digital camera. The phase composition of the parts sintered was determined with x-ray diffraction (XRD) using a DRON-3 diffractometer in Cu-K_α radiation. The morphology of the HA coating on nitinol after SLS/SLM was studied with a LEO 1450 scanning electron microscope (Carl Zeiss Company) equipped with an energy-dispersive x-ray analyzer (INCA Energy 300, Oxford Instruments).

RESULTS AND DISCUSSION

The shape of particles and the method of their formation influence both the conditions in which the starting powder is leveled and the result of layer-by-layer sintering (density). The number of closed pores depends on the process used to produce the powder (atomization, fragmentation, chemical vapor deposition). Nonatomized (nonspherical) particles are characterized by electrostatic charge that is unevenly distributed on their surface and leads to their agglomeration. When such particles are leveled with a roller, grooves tend to form over the powder, so spherical particles are more preferable.

Figure 2*a* shows that the starting nitinol particles are spherical. The surface of individual particles is smooth, with minor concaves and convexities about 1–10 μm in height. Particles of the hydroxyapatite powder (Fig. 2*b*) produced by the TLS Technik GmbH&Co are flaky, elongated, and probably dendritic (Fig. 2*c*). The individual substructural threads are 70 to 80 nm in size (Fig. 2*c*). The elemental composition of the powders corresponds to the manufacturer's standard.

Figure 3 shows individual single layers subjected to SLS (PM-100 setup) in loose powder whose thickness is greater than the sintering depth of one single layer. The sintering depth increases with laser energy input into the

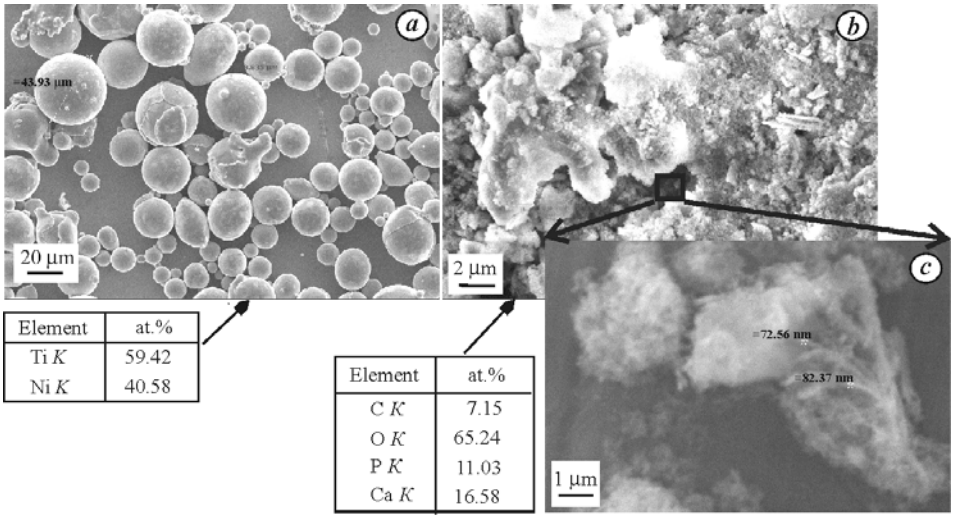

Fig. 2. SEM image of NiTi (*a*) and HA (*b*, *c*) starting powders and EDX data averaged over the entire image (tables)

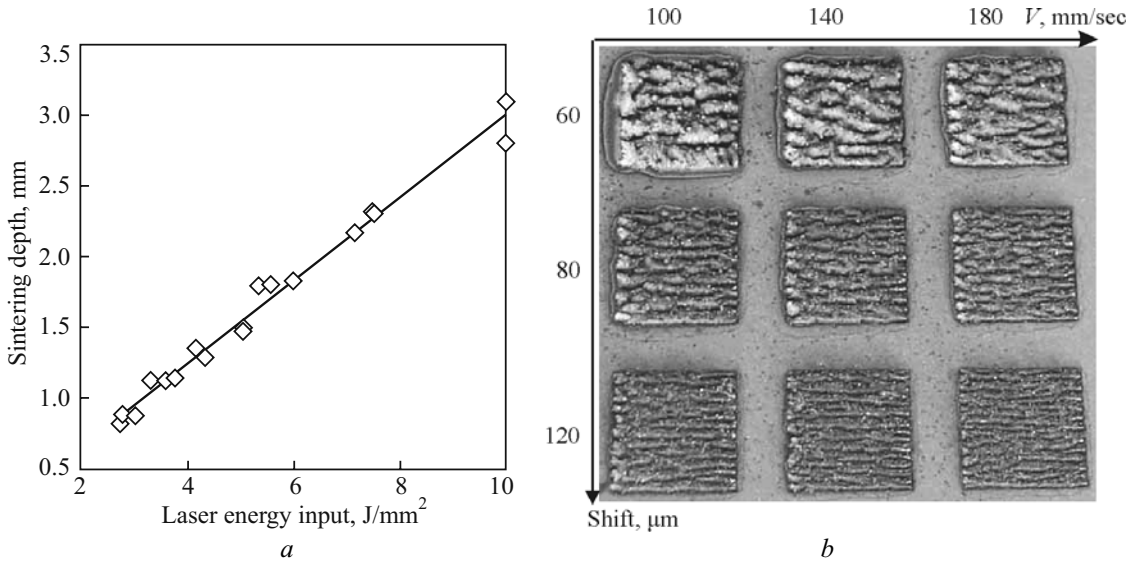

Fig. 3. Laser (single-band) sintering (at T = 25°C in the chamber) of an individual single layer over the surface of loose powder: *a*) sintering depth of a single layer depending on surface laser energy input; *b*) appearance (top view) of individual single layers (10 × 10 mm, NiTi (–45 μm)) in the powder; the thickness of single layers is shown in Fig. 3*a*

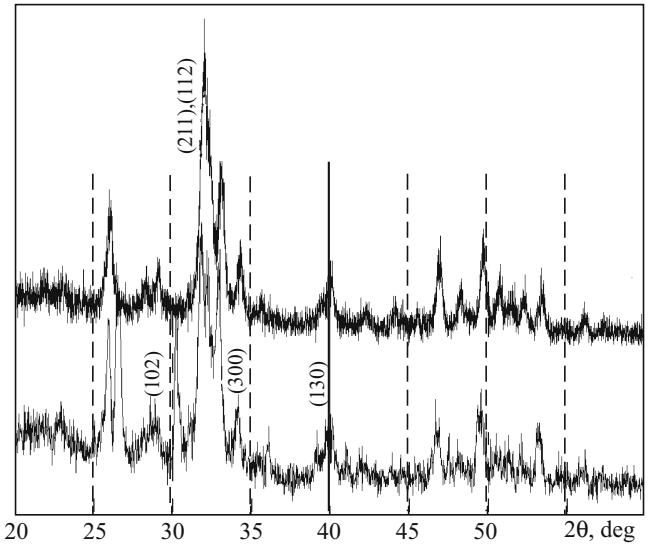

Fig. 4. X-ray diffraction of HA powder before (bottom) and after (top) SLS: laser parameters: laser scanning rate V = 1.5 cm/sec, spot diameter ~100 μm, and laser power P = 25.8 W

powder (Fig. 3*a*). Figure 3*b* shows the appearance of porous single layers in the starting (prior to treatment) powder. At a constant power of 50 W (Fig. 3*b*), the sintered surface of a single layer becomes rougher with decreasing laser scanning rate and with decreasing spacing between passes of the laser beam (shift parameter). For a shift of 60 μm and a scanning rate of 100 mm/sec, there is a clear area around the sintering zone which was also heated to high temperatures, leading to sticking of the powder left after SLS. Therefore, SLS involving a 120 μm shift is preferred for layer-by-layer SLS in terms of production effectiveness and quality.

It is reported in [2] that, unlike furnace sintering, high-speed SLS does not cause HA ceramics and individual components, $Ca_4P_2O_9$ and $Ca_3(PO_4)_2$, to decompose into individual phases: α, β-TCP (tricalcium phosphate), P_2O_5, CaO, $CaTiO_3$, and Ti_3P, in the presence of nitinol. It is believed that the α, β-TCP, $Ca(H_2PO_4)_2$,

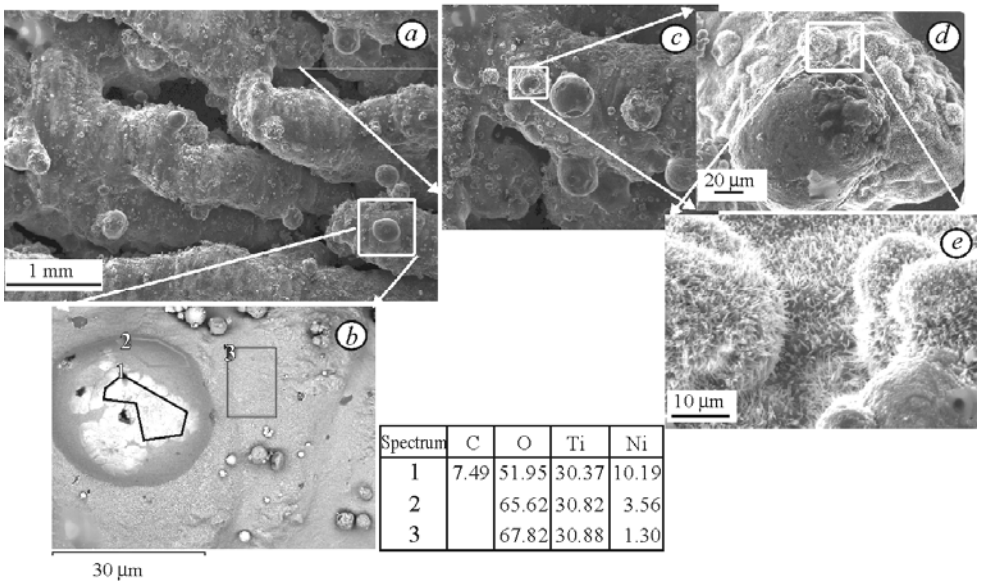

Spectrum	C	O	Ti	Ni
1	7.49	51.95	30.37	10.19
2		65.62	30.82	3.56
3		67.82	30.88	1.30

Fig. 5. Micro- and submicron structures on nitinol surface after SLM according to SEM: *a*, *c*) interconnected porosity; *d*, *e*) highly developed surface topology; for areas 1, 2, and 3 (Fig. 5*b*) the table shows low amount of free nickel according to EDX analysis

and $CaHPO_4$ phases retain the pharmacological properties of the starting ceramics [10, 19]. X-ray diffraction of HA ceramics before and after SLS (Fig. 4) confirmed the presence of the crystalline HA phase and lines of β-TCP [20]. The two diffraction spectra correspond exactly to the JCPDS reference file for HA. The main intensity peaks for crystalline HA are at 31.83, 32.10, and 32.90°. The broadening at low 2θ angles corresponds to the amorphous/nanostructured HA phase. The intensity of the peaks changes insignificantly after laser treatment. In general, high-speed laser treatment hardly changes the distribution of diffraction peaks. That means that, unlike prolonged furnace heating, short-term laser treatment has no effect on the structural and phase composition of HA ceramics.

The surface morphology of nitinol after SLM is shown in Fig. 5. The surface structure with deep grooves (Fig. 5*a*) is a convenient medium for connective tissues to integrate with the implant. Inclusions of molten nitinol about 100 μm in size are clearly visible on the surface of these grooves. Higher magnification (Fig. 5*d, e*) shows that the surface of the sample has developed nanostructure. Energy-dispersive x-ray analysis of areas 1–2–3 (Fig. 5*b*) leads us to suggest, relying on the stoichiometry, that there are titanium oxides and oxynitrides. The amount of nickel on the surface is minimum. This obviously explains the successful application of SLS-produced nitinol parts as implant materials in [3, 18, 19]. The study [20] shows that a small amount of nickel on the surface is associated with more than just active oxidation of titanium when nitinol is heated. The complex structure of interconnected pores and the multilayered surface make it difficult to evaluate the actual amount of nickel.

X-ray diffraction shows that, besides NiTi, other intermetallic phases binding free nickel, $NiTi_2$ and Ni_3Ti, are also prone to form. With increasing laser power, the conditions for their formation become favorable. To determine the effect of HA coating on the SLS/SLM process, the samples were subjected to XRD (Fig. 4). The diffraction peaks of the nitinol substrate at an angle of 42° and the broadened peaks between 31 and 33° can be interpreted as interplanar (211), (112), and (300) lines of HA. Great laser energy input leads to intensive recrystallization of molten nitinol (SLS (*b, d, e*) and SLM (*a, c*) results in Fig. 6) and activation of oxidative processes on the nitinol surface (energy-dispersive x-ray analysis). It can be assumed that the hydroxyapatite coating over nitinol restricts the release of nickel to the surface. The Ca/P ratio in areas 1–2 (Fig. 6*b*) and area S1 (Fig. 6*d*), according to energy-dispersive x-ray analysis, meets the requirements of biocompatibility. Meanwhile, excessive hydroxyapatite affects the conditions of nitinol laser sintering: the structure becomes more brittle following SLS and SLM and porosity increases after sintering at a laser power of 13.6 W.

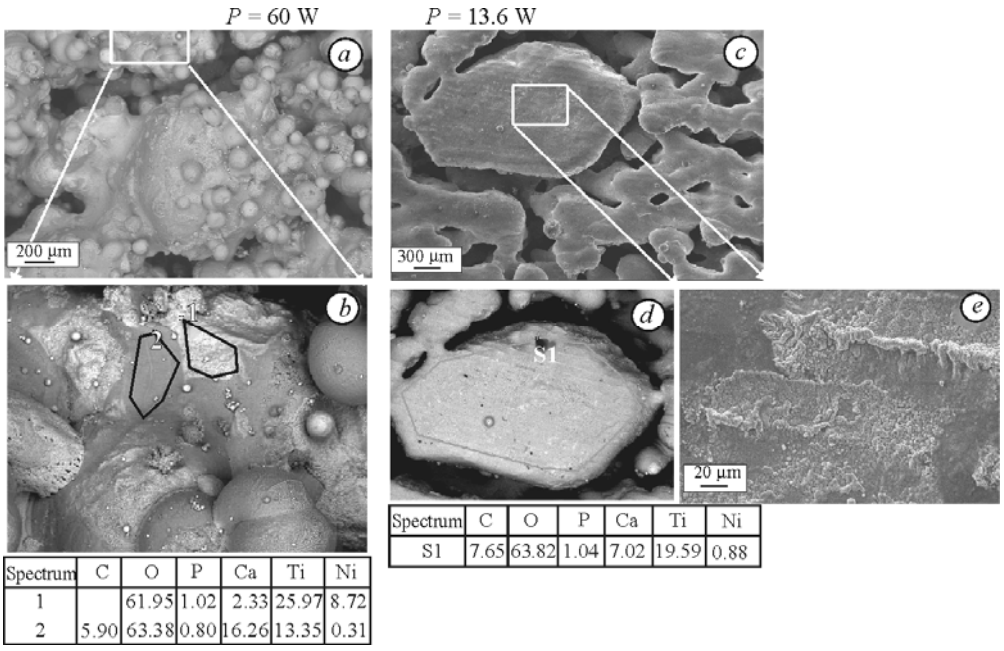

Spectrum	C	O	P	Ca	Ti	Ni
1		61.95	1.02	2.33	25.97	8.72
2	5.90	63.38	0.80	16.26	13.35	0.31

Spectrum	C	O	P	Ca	Ti	Ni
S1	7.65	63.82	1.04	7.02	19.59	0.88

Fig. 6. SEM microphotographs of NiTi + HA surface: *a*, *b*) laser melting; *c*, *d*, *e*) laser sintering

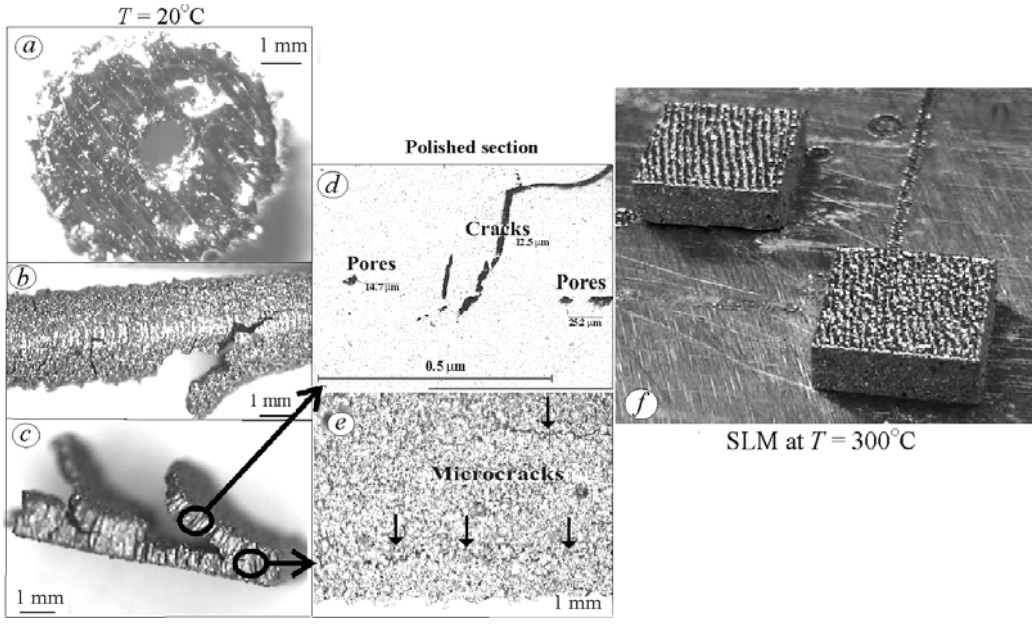

Fig. 7. SLM of 3D nitinol parts at different temperatures in the synthesis chamber: *a*) end face of a nitinol pin; *b*) lateral side of a nitinol pin; *c*) thin wall, *d*, *e*) nucleation of microcracks; *b*, *c*) macrolamination of 3D parts; *a*, *f*) result of successive SLM

The common issue in using the porous structures resulting from SLS/SLM in tissue engineering is a tendency to the necrosis of tissues at edges and protrusions [21]. This issue can be solved through special surface micro- and nanoarchitecture and increase in biocompatibility with HA additions. Being closely similar to the mineral phase of the bone, HA ceramics improve the exchange of nutrients and cell adhesion from the surface to the center of a porous nitinol implant. The SLS/SLM technique can actually be used to promote controlled (gradient) architecture of pore channels in a part even at the stage of computer simulation.

As noted above, excessive HA impairs the strength properties of a NiTi implant. Cracks form and propagate even during SLM of pure nitinol (Fig. 7). Residual stresses induced by high-speed heating and cooling

during selective laser melting at room temperatures cause the stratification of 3D parts. Layer-by-layer synthesis at room temperatures has resulted in cylindrical 3D parts of good quality, probably because of the balanced redistribution of thermal stresses (Fig. 7*a*). However, cold cracks propagate over a pin as it cools down in the synthesis chamber. These cracks result from the slow unloading of the material after elastoplastic deformation induced during SLM. The emerging residual stresses lead to a relative shift of intermetallic grains along the boundary, giving rise to cracks at these boundaries (Fig. 7*b–e*). In this connection, we recommend combining the process of selective laser melting with additional heating of powder in the chamber up to 300–500°C (Fig. 7*f*), which has led to a favorable effect.

Note that the optimization of selective laser melting of more complex nitinol parts requires further study.

CONCLUSIONS

X-ray diffraction, optical and electron microscopy, and energy-dispersive x-ray analysis are used to determine parameters of selective laser sintering/melting of a hydroxyapatite ceramic–nitinol intermetallic system. It can be stated that the SLS/SLM technique is suitable for producing porous and full-density 3D parts from a biocompatible material, nitinol, including HA additions. Experiments have revealed no significant decomposition of HA under laser treatment and have shown that the main pharmacological properties of the ceramics are retained (judging from the Ca/P ratio). Additional oxidation of free titanium during SLS/SLM reduces the amount of nickel released to the surface of parts. The formation of a HA ceramic layer over the porous NiTi surface also restricts the release of free nickel but increases the brittleness of parts. Preliminary computer simulation of pore channel microarchitecture should promote biocompatibility by improving the exchange of nutrients and cell adhesion from the surface to the center of a porous nitinol implant. These intelligent parts can be used on nonstressed areas of the human body as engineered tissue structures, cellular matrices, and porous drug delivery systems.

It is shown that layer-by-layer synthesis of high-quality full-density 3D parts is a challenge because cracks develop during and after the process. Selective laser melting, which combines the SLM process and additional heating of the powder to 300–500°C, has been employed to manage the creation a full-density 3D part. These full-density samples can be used not only as scaffolds but may also be applied to stressed skeleton areas in maxillofacial surgery, orthopedics, and trauma recovery.

ACKNOWLEDGEMENT

The research has been sponsored through the Russian Fundamental Research Fund (Project No. 10-08-00208-a) and a grant under the Program “Fundamental Sciences for Medicine” (Stages 2009–2011) of the Presidium of the Russian Academy of Sciences.

REFERENCES

1. I. V. Shishkovsky, D. M. Gureev, and A. L. Petrov, “Formation of intermetallic phases under laser sintering of powdered SHS compositions,” *Proc. SPIE*, **3688**, 237–242 (1999).
2. I. V. Shishkovskii, L. V. Zhuravel’, A. L. Petrov, and E. Yu. Tarasova, “Synthesis of biocomposite based on NiTi with hydroxyapatite during selective laser sintering,” *Pis’ma Zh. Tekh. Fiz.*, **27**, No. 5, 81–86 (2001).
3. I. V. Shishkovsky, L. T. Volova, M. V. Kuznetsov, et al., “Porous biocompatible implants and tissue scaffolds synthesized by selective laser sintering from Ti and NiTi,” *J. Mater. Chem.*, **18**, No. 12, 1309–1317 (2008).
4. S. Shabalovskaya, J. Anderegg, and J. Van Humbeeck, “Critical overview of Nitinol surfaces and their modifications for medical applications,” *Acta Biomater.*, **4**, 447–467 (2008).
5. H. C. Jiang and L. J. Rong, “Effect of hydroxyapatite coating on nickel release of the porous NiTi shape memory alloy fabricated by SHS method,” *Surf. Coat. Technol.*, **201**, 1017–1021 (2006).

6. V. Muhonen, R. Heikkinen, A. Danilov, et al., “The effect of oxide thickness on osteoblast attachment and survival on NiTi alloy,” *J. Mater. Sci.: Mater. Med.*, **18**, No. 5, 959–967 (2007).
7. S. Eosoly, S. Lohfeld, and D. Brabazon, “Effect of hydroxyapatite on biodegradable scaffolds fabricated by SLS,” *Key Eng. Mater.*, **396–398**, 659–662 (2009).
8. R. D. Goodridge, D. J. Wood, C. Ohtsuki, and K. W. Dalgarno, “Biological evaluation of an apatite–mullite glass-ceramic produced via selective laser sintering,” *Acta Biomater.*, **3**, 221–231 (2007).
9. C. K. Chua, K. F. Leong, K. H. Tan, et al., “Development of tissue scaffolds using selective laser sintering of polyvinyl alcohol/hydroxyapatite,” *J. Mater. Sci.: Mater. Med.*, **15**, 1113–1121 (2004).
10. B. Duan, M. Wang, W. Y. Zhou, and W. L. Cheung, “Synthesis of Ca–P nanoparticles and fabrication of Ca–P/PHBV nanocomposite microspheres for bone tissue engineering applications,” *Appl. Surf. Sci.*, **255**, 529–533 (2008).
11. C. Von Wilmowsky, E. Vairaktaris, D. Pohle, et al., “Effects of bioactive glass and β-TCP containing three-dimensional laser sintered polyetheretherketone composites on osteoblasts in vitro,” *J. Biomed. Mater. Res.*, **87**, No. 4, 896–902 (2008).
12. J. L. Arias, M. B. Mayor, F. J. G. A Sanz, et al., “Structural analysis of calcium phosphate coatings produced by pulsed laser deposition at different water-vapor pressures,” *J. Mater. Sci.: Mater. Med.*, **8**, 873–876 (1997).
13. K. W. K. Yeung, R. Y. L. Chan, K. O. Lamand, et al., “In vitro and in vivo characterization of novel plasma treated nickel titanium shape memory alloy for orthopedic implantation,” *Surf. Coat. Technol.*, **202**, 1247–1251 (2007).
14. Z. D. Cui, M. F. Chen, L. Y. Zhang, et al., “Improving the biocompatibility of NiTi alloy by chemical treatments: An in vitro evaluation in 3T3 human fibroblast cell,” *Mater. Sci. Eng. C*, **28**, 1117–1122 (2008).
15. I. V. Shishkovsky, “Synthesis of functional gradient parts via RP methods,” *Rapid Prototyping J.*, **7**, No. 4, 207–211 (2001).
16. I. Yadroitsev, Ph. Bertrand, B. Laget, and I. Smurov, “Application of laser assisted technologies for fabrication of functionally graded coatings and objects for the international thermonuclear experimental reactor components,” *J. Nucl. Mater.*, **362**, 189–196 (2007).
17. J.-P. Kruth, P. Mercelis, J. Van Vaerenbergh, et al., “Binding mechanisms in selective laser sintering and selective laser melting,” *Rapid Prototyping J.*, **11**, 26–36 (2005).
18. I. V. Shishkovsky, M. V. Kuznetsov, and Yu. G. Morozov, “Porous titanium and nitinol implants synthesized by SHS/SLS: microstructural and histomorphological analyses of tissue reactions,” *Int. J. Self-Propag. High-Temp. Synth.*, **19**, No. 2, 157–167 (2010).
19. I. V. Shishkovskii, *Laser Synthesis of Functional Mesostructures and 3D Parts* [in Russian], Fizmatgiz, Moscow (2009).
20. H. C. Jiang and L. J. Rong, “Effect of hydroxyapatite coating on nickel release of the porous NiTi shape memory alloy fabricated by SHS method,” *Surf. Coat. Technol.*, **201**, 1017–1021 (2006).
21. F. R. Rose, L. A. Cyster, D. M. Grant, et al., “In vitro assessment of cell penetration into porous hydroxyapatite scaffolds with a central aligned channel,” *Biomater.*, **25**, 5507–5514 (2004).